Polymer Journal (2017) 49, 391–399

www.nature.com/pj

ORIGINAL ARTICLE

# *In situ* polymerized polyaniline nanofiber-based functional cotton and nylon fabrics as millimeter-wave absorbers

Nina Joseph[1,2], Jobin Varghese[1,2] and Mailadil Thomas Sebastian[1,2]

**Polyaniline nanofibers and their composite with graphite have been synthesized by a simple chemical polymerization method. Polyaniline nanofiber graphite composites with a thickness of 1 mm exhibit excellent electromagnetic interference (EMI) shielding of above 80 dB in the frequency range of 8.2–18 GHz. EMI shielding fabrics of 0.1 mm thickness based on polyaniline nanofibers and their composite have been developed by an *in situ* polymerization route. These fabrics combine the properties of polyaniline nanofibers as well as their composite and fabrics (cotton and nylon). The developed functional fabrics with 0.1 mm thickness exhibit EMI shielding effectiveness in the range of 11–15 dB in the 8.2–18 GHz frequency range. Optical and scanning electron microscopy studies indicate the uniform coating of the polyaniline nanofibers over the individual fibers and interweave regions. Thin and flexible shielding materials suitable for a broad range of millimeter-wave shielding applications have been developed using this simple and potentially profitable method.**
*Polymer Journal* (2017) **49,** 391–399; doi:10.1038/pj.2016.121; published online 4 January 2017

## INTRODUCTION

The recent growth of electronics and instrumentation around the world has caused electromagnetic interference (EMI), which is now becoming a vital concern in the millimeter-wave frequency ranges. EMI is a form of electromagnetic pollution that can cause disturbances, including faulty operation of appliances or leakage of information. Exposure to electromagnetic waves (EM) can also affect human health. EMI can cause adverse effects on all contemporary electrical and electronic systems, from those used in daily life to those applied in space exploration, and can result in losses of money, energy, time and even life.[1–3] Hence, there is an urgent need for suitable and efficient EMI shielding materials for millimeter-wave applications. Various methods have been employed to develop lightweight and efficient EMI shielding materials to increase the device lifetime and efficiency. Shielding against EMI is achieved by reflection or absorption or a combination of the two mechanisms. Low-frequency EM radiation can be shielded against by reflection mechanism, whereas millimeter waves can be attenuated by absorption. Millimeter-wave EM absorbers are an important area of current research due to their growing demand in various spheres of life. Moreover, thin and flexible shielding materials can provide the additional benefits of being user-friendly, inexpensive and able to be used on surfaces of all shapes. Conductive fabric-based shielding materials can serve these purposes. These materials can provide flexibility, excellent formability and mechanical properties, EM discharge and EMI protection, RF interference protection, and thermal expansion matching while also being lightweight.[4–6] The recent primary applications of conducting fabrics include filters, EMI shielding materials, and antibacterial and flame-retardant materials.[7] These fabrics can find applications as shielding materials in aerospace and the military, electronics and medical equipment. They can provide grounding, shielding and electromagnetic compatibility to radio frequency interference from ground sensitive electronic components and boards, cables, sensors, FM/AM radios, wireless phones, cellular phones and computers that operate at up to 1000 MHz frequency. Fabrics with low EMI shielding effectiveness (SE) value, less than required for commercial EMI shielding applications, are suitable for shielding electrostatic discharge (ESD).[3,8,9]

Traditional EMI shielding materials rely on metallic materials to effectively shield against unwanted radiation. Gupta *et al.*[10] reported hybrid woven fabrics having a stainless steel/polyester composite yarn of a thickness of approximately 0.4 mm with an EMI SE of 31 dB in the frequency range of 8–18 GHz. Metal coating is another approach to obtain good shielding materials. Shinagawa *et al.*[11] performed the electroless plating of Cu and Ni on paper and synthetic pulp. The metal-coated paper exhibits 40 dB SE between 10 MHz and 1 GHz. Kumar *et al.*[12] reported an EMI SE of 58.7 dB for carbon–copper (C–Cu) nanocomposites produced by coating nanocrystalline Cu on heat-treated polyaromatic hydrocarbons of 2-mm thickness in the Ku-band frequency range. Perumalraj and Dasaradhan[13] prepared

[1]Materials Science & Technology Division, CSIR NIIST, Thiruvananthapuram, India and [2]Microelectronics Research Unit, Faculty of Information Technology and Electrical Engineering, University of Oulu, Oulu, Finland
Correspondence: Dr MT Sebastian, Microelectronics Research Unit, Faculty of Information Electrical Engineering and Information Technology, University of Oulu, Oulu 90570, Finland.
E-mail: mailadils@yahoo.com
Received 4 August 2016; revised 15 November 2016; accepted 16 November 2016; published online 4 January 2017

fabric from a nickel-plated copper core conductive yarn with an EMI SE of 25–45 in the frequency range of 200–1000 MHz. Carbon-based shields are also widely used due to their flexibility, corrosion resistance, lightweight and formability.[14–19] Non-woven polyester and knitted cotton fabric coated with multiwalled carbon nanotubes, multiwalled carbon nanotubes+silver nanoparticles, multiwalled carbon nanotubes+nickel-coated carbon fibers and nickel-coated carbon fibers of 100–200-μm thickness show EMI SE values in the range of 9–19 dB at 1 GHz.[20] Hence, the current technology uses mainly metal/carbon shielding, which can provide excellent EMI SE. In spite of their superior shielding performance, metal-coated fabrics have many drawbacks such as reduced wear and scratch resistance, poor mechanical properties, high rigidity, heavy weight, corrosion susceptibility, processing cost and shielding predominantly by reflection. On the other hand, the use of carbon fillers exhibits problems of cost, sloughing, and health and long-term environmental issues that limit their application as shielding materials for many practical applications.[4,21–23] Magnetic structures can exhibit effective absorption in the high-frequency range due to their high magnetization, but their weak magnetocrystalline anisotropy decrease in permeability due to ferromagnetic resonance, and eddy current losses induced by EM waves at high frequencies, especially in the gigahertz region, limit their application for EM wave absorption. Hence, proper modification of the magnetic fillers is needed to achieve good shielding performance.[24–26]

Intrinsically conducting polymers with finite conductivity and non-transparency to microwaves can provide an attractive solution to solve this problem and deliver a new generation of EMI shielding for many millimeter-wave applications.[27–32] Notably, the conducting polymer polyaniline and its composites are garnering considerable attention because of their attractive electrical, thermal and mechanical properties as well as low density, tunable conductivity, non-corrosiveness, nominal cost, ease of synthesis, shielding by absorption rather than reflection, better ESD and environmental stability, resulting in their potential use in the full range of techno-commercial applications.[28,33–36] Hence, polyaniline can have a future critical scope in the communications industry as a shielding material.[36] Despite such exciting properties, its commercial utility is limited due to its poor mechanical properties, which result from the rigid characteristics imbued by the chemical conformation of its benzene rings.[28,37,38] Several efforts have been made to design a conducting polymer as a flexible and extensive-area EMI shield.[39–41] A simple approach to obtain thin and flexible shielding materials based on conducting polymers such as polyaniline is by developing conducting fabrics. Such materials combine the mechanical properties, stretch and flexibility of fabrics with the conductivity of the polymer and have been reported to be suitable for many applications in the electronics and communications industry.[3,22,28,31,42–46] Polyaniline-based fabrics have been reported for appropriate applications such as fibrous sensors, smart clothing and EMI shielding, as well as antistatic discharge applications such as the packaging of microelectronic devices.[22,23,31,44,45] These fabrics can be used as EMI-shielded cloth for concerned persons and radar shields in the military as well as heat-generating fabrics for devices.[23] Such fabrics can be prepared either by coating conducting polymers or by the *in situ* polymerization of various monomers.[7] All reported preparation protocols of conducting fabrics based on polyaniline involve many surfactants and solvents, as well as a tedious preparation process, which make it less economically viable.[22,23,31] Hence, cheap, thin and flexible EMI shields are needed for present and future applications in the communications and electronics industry. The present work is an attempt to develop EMI shielding conducting cotton and nylon fabrics based on polyaniline nanofibers and their composites by a simple *in situ* polymerization route. The synthesis method involves no surfactant or chemical solvent and yields polyaniline nanofibers of excellent conductivity and EMI shielding effectiveness.[47] The fibrillar morphology of the synthesized polyaniline provides an added advantage to the flexibility and stability of the developed fabrics. The polyaniline nanofiber composite was prepared by the addition of graphite flakes (Gp) during the polymerization of the polyaniline nanofibers.

## EXPERIMENTAL PROCEDURES

### Synthesis

*Synthesis of polyaniline nanofibers and polyaniline nanofiber graphite composite.* The polyaniline nanofibers (P) were synthesized by the polymerization of aniline hydrochloride monomers (Alfa Aesar, Ward Hill, MA, USA) using ammonium persulfate (Aldrich Chemical Company, Inc., Milwaukee, WI, USA) as the reducing agent. The synthesis was achieved by the dropwise addition of ammonium persulfate dissolved in 1 M HCl into an aniline hydrochloride solution in 1 M HCl at an oxidant monomer molar ratio of 1.15 at room temperature. The reaction mixture was kept stable for 36 h to facilitate the growth of uniform polyaniline nanofibers. The resulting green precipitate was filtered and washed with water and methanol to remove excess acids and by-products from the polymerization. The obtained green powder was then dried in a vacuum oven at 60 °C for 24 h.[43]

The graphite filler incorporated polyaniline nanofiber composite (GpP) was prepared in a manner similar to that of pure polyaniline nanofibers with the additional component of graphite flakes (Gp Carborundum Universal, Ltd, Mumbai, India). The molar ratio of aniline hydrochloride to filler (Gp) in the preparation of GpP was 1:4, that is, approximately 2.3 weight% (wt.%) Gp in P.

*Synthesis of polyaniline nanofibers and their graphite composite-based cotton and nylon fabrics.* The polyaniline-based fabrics were prepared by the *in situ* polymerization of aniline hydrochloride. The cotton or nylon fabrics were dipped in the aniline monomer solution for 24 h, and the polymerization was carried out by the dropwise addition of ammonium persulfate followed by keeping the reaction mixture stable for 36 h, similar to the synthesis of the polyaniline nanofibers,[47] as schematically represented in Figure 1. The formation of the coating of polyaniline nanofibers on the surface of the fabrics during the polymerization was marked by the appearance of a green color. The fabrics were removed from the solution, washed with methanol and dried in a vacuum oven at 60 °C for 24 h.

### Characterization

The phase formation was determined using an X-ray diffraction (XRD) pattern using CuKα radiation (X'Pert PRO MPD X-ray diffractometer; PANalytical, Almelo, Netherlands) in the $2\theta$ value range of 10–90°. The morphologies of the synthesized polyaniline nanofibers and composite were studied using a transmission electron microscope (FEI Tecnai-G2 30S-TWIN; FEI Company, Hillsboro, OR, USA). The ultraviolet–visible absorption of the polyaniline nanofibers and their graphite composite was measured using a Shimadzu 3600 UV-vis-NIR spectrophotometer. The photographic images were recorded with a digital camera (Sony, ×10 optical zoom, 16 M pixels, Tokyo, Japan) and the visual images by optical microscopy (Leica, MRDX, Wetzlar, Germany). The surface morphology of the fabrics based on the synthesized polyaniline nanofibers was analyzed using a scanning electron microscope (SEM, JEOL, JSM-5600LV, Tokyo, Japan). The EMI shielding measurements were performed by the waveguide method, connected to a vector network analyzer (Agilent Technologies, Mississauga, ON, Canada, E5071C, ENA series, 300 kHz-20 GHz, CA) with samples of dimensions 22.86 × 10.80 mm for the X-band (8.2–12.4 GHz) and 15.80 × 7.90 mm for the Ku-band (12.4–18 GHz) frequency ranges. The polyaniline nanofibers and their composite were pressed into a sample of thickness 1 mm for the EMI shielding measurements.

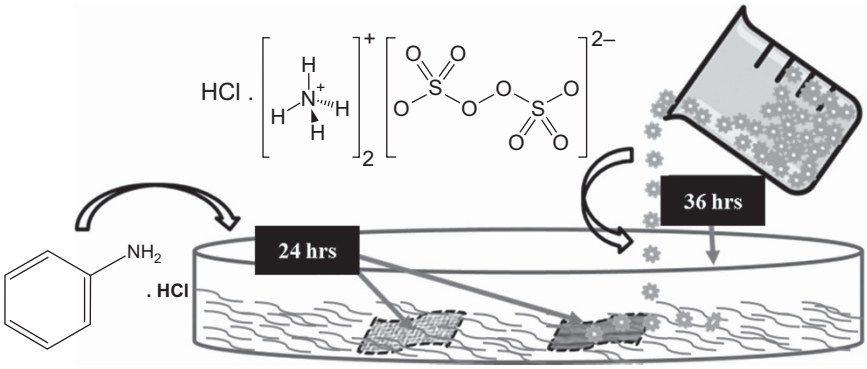


**Figure 1** Schematic representation of the preparation of functional cotton and nylon fabrics based on polyaniline nanofibers and their composite. A full color version of this figure is available at *Polymer Journal* online.

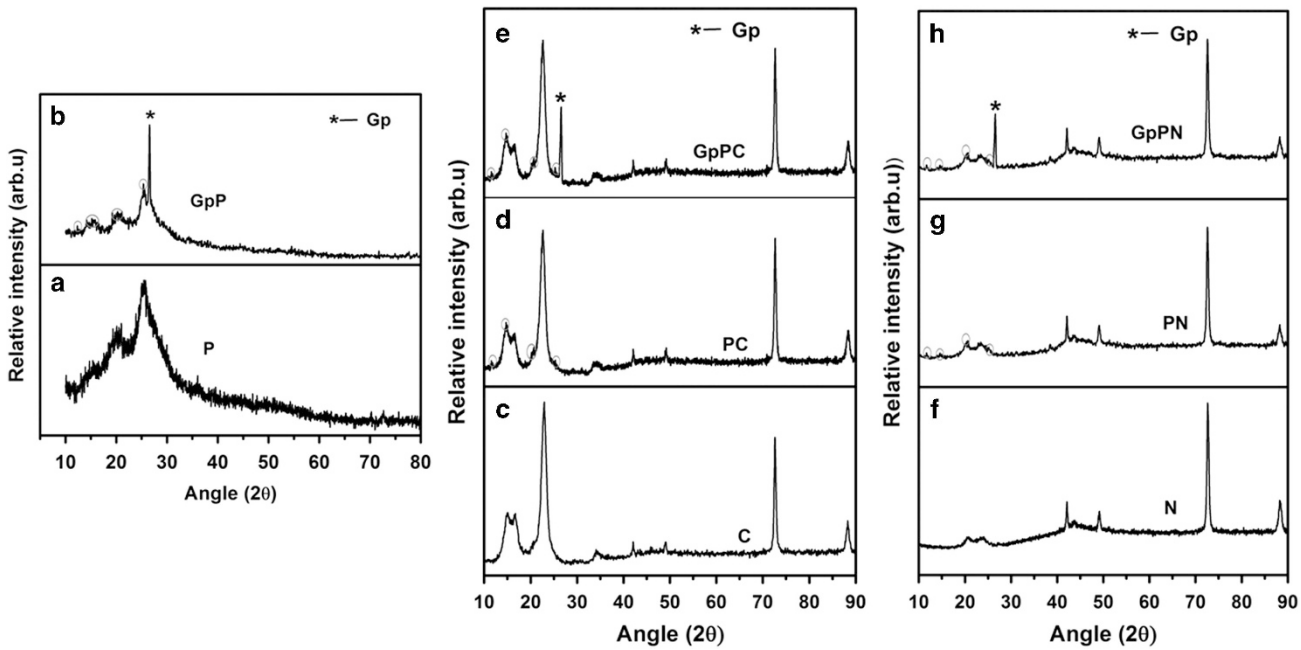


**Figure 2** XRD patterns of (**a**) polyaniline nanofiber (P), (**b**) polyaniline nanofiber graphite composite (GpP), (**c**) pure cotton (C), (**d**) polyaniline nanofiber-based cotton (PC), (**e**) polyaniline nanofiber graphite composite-based cotton (GpPC), (**f**) pure nylon (N), (**g**) polyaniline nanofiber-based nylon (PN) and (**h**) polyaniline nanofiber graphite composite-based nylon (GpPN) fabrics. A full color version of this figure is available at *Polymer Journal* online.

## RESULTS AND DISCUSSION

The cotton fabrics based on the P and GpP composites are designated PC and GpPC, respectively, while the corresponding nylon fabrics are designated PN and GpPN, respectively. The XRD patterns of the polyaniline nanofibers (P) and polyaniline nanofiber graphite composite (GpP) are depicted in Figures 2a and b, respectively. Figures 2d and e depict the XRD pattern of pure cotton fabric (C), as well as those of polyaniline nanofiber and polyaniline nanofiber graphite composite-based cotton fabrics, respectively. The polyaniline nanofibers have peaks at $2\theta$ values of approximately 11°, 15°, 20° and 25°. The presence of the crystalline phase of the polyaniline nanofibers indicates the metallic conductive state.[48] The peaks observed near 15° and 25° are crystalline peaks and that observed at 20° is the amorphous peak of polyaniline.[49] The XRD pattern of the polyaniline nanofiber graphite composite (GpP) clearly reveals the presence of graphite in the polyaniline nanofiber matrix. It also indicates that the interactions between the polyaniline nanofibers and graphite are purely physical. The diffraction peaks observed in the XRD pattern of the pristine cotton fabric are related to the crystalline structure of cellulose I.[50–52] The peaks of the polyaniline nanofibers are not clearly visible in the XRD pattern of the polyaniline nanofiber and polyaniline nanofiber graphite composite-based cotton fabrics, as they overlap with the high-intensity peaks of the cotton fabrics. The peaks can be seen when carefully examining the XRD patterns and are marked for greater clarity. The peaks at $2\theta = 26.5°$ in the XRD pattern of the polyaniline nanofiber graphite composite-based cotton fabrics correspond to the graphite phases from the (002) reflection and indicate the good coating of the polyaniline nanofiber graphite composite over the cotton fabrics.[53] The successful growth of the polyaniline nanofibers and polyaniline nanofiber graphite composite can be seen from the

XRD patterns shown in Figures 2d and e. Similarly, the XRD patterns of pure nylon fabrics (N) and polyaniline nanofiber and polyaniline nanofiber graphite composite-based nylon fabrics are presented in Figures 2f–h, respectively.[54,55] Compared with the XRD pattern of pristine nylon fabrics, a few new peaks corresponding to the polyaniline nanofibers and polyaniline nanofiber graphite composite are observed in the XRD pattern and are marked. This clearly demonstrates the presence of the polyaniline nanofibers and polyaniline nanofiber graphite composite on the nylon fabrics. The growth of the polyaniline nanofibers and polyaniline nanofiber graphite composite on the fabrics (both cotton and nylon) is evident from their XRD patterns and from the green color of the coated fabrics shown in the photographic images (Figures 4b and d).

Figures 3a–c depict transmission electron microscopy images of the graphite flakes, polyaniline nanofibers and polyaniline nanofiber graphite composite, respectively. It is evident from the figure that the graphite has a flake-like morphology of a few nanometers in thickness, while the polyaniline nanofibers exhibit a fibrillar morphology of approximately 200 nm in diameter. The transmission electron microscope image of the polyaniline nanofiber graphite composite (Figure 3c) indicates that a conducting polyaniline nanofiber composite is obtained by the uniform distribution of graphite filler in the polyaniline matrix.

The solid-state absorption spectra of the polyaniline nanofibers and polyaniline nanofiber graphite composite are shown in Figure 3d. There are two bands attributed to the $\pi$–$\pi^*$ transition within the benzenoid segment and n–$\pi^*$ transitions within the quinoid structure. This indicates the presence of localized polaronic states such that the synthesized polyaniline nanofibers are in the emeraldine salt form.[47] A slight shift can be observed in the bands of the ultraviolet–visible spectra of the polyaniline nanofiber graphite composite, which may be due to the formation of a charge transfer complex between the doped polyaniline nanofibers and graphite.[56] This eventually leads to good conductivity as well as high EMI shielding efficiency in the composite. Hence, the presence of graphite impacts the conductivity and hence the EMI shielding property of the polyaniline nanofibers.

Photographs of the pristine and polyaniline nanofiber grown fabrics are shown in Figures 4a–d. The pristine cotton (Figure 4a) and nylon (Figures 4c) fabrics are white, but after the growth of the polyaniline nanofibers, the colors of both fabrics change to green, as shown in Figure 4b and d, respectively. The color change indicates that the coating of the polyaniline nanofibers is extended over the entire cotton and nylon fabric samples. The growth of the nanofibers is further confirmed by the optical and SEM images of the coated and uncoated fabrics. The mesh openings of both the pristine cotton and nylon fabrics are clearly seen in the optical images shown in Figures 5a and c, respectively, as well as the SEM images depicted in Figures 6a and c, respectively. The mesh openings cannot be seen in the optical images of the polyaniline nanofiber-based cotton and nylon fabrics shown in Figures 5b and d, respectively. This observation reveals that thin coatings of polyaniline nanofibers in the few-micrometer range are formed over the fabrics. Similar observations were obtained from the SEM images of the polyaniline nanofiber-based cotton and nylon fabrics, as shown in Figure 6b and d, respectively. It is evident from the SEM images that the polyaniline nanofibers are uniformly formed over the fabrics, producing uniform coatings. The fibrillar morphology of the polyaniline is observed to be maintained even after the coating. This is due to the consistent growth of the polyaniline nanofibers over the fabrics as they were dipped in the monomer solution for approximately 24 h, which results in the uniform coating of the aniline monomer over the fabrics followed by a stable reaction time of 36 h. A reaction time less than 36 h does not provide uniform coatings, and relatively little polyaniline was coated on the fabrics. In addition, the fibrillar morphology of the polyaniline is not well maintained using a low reaction time, as reported in our earlier work,[47] and all of these factors will result in a low EMI shielding effectiveness. A higher reaction time provides a larger polyaniline coating thickness, which delaminates while washing or drying the fabrics. Hence, only a small amount of polyaniline coating can be achieved, resulting in a low EMI shielding effectiveness. The polyaniline nanofibers coated over the fabrics during 36 h of reaction time are uniform and do not exhibit delamination, as is evident from the s.e.m. images. The addition of a reducing agent leads to the consistent and uniform growth of the polyaniline nanofibers over the fabrics due to the combined effect of all of the reaction conditions.[47] The presence of acid guides the self-assembled growth of the nanofibers by helping the monomer to form micelles, while the room temperature facilitates the reaction process and the stable reaction condition prevents the secondary growth of polyaniline. The fabrics thus act as substrates for the growth of polyaniline nanofibers, which provide a conducting coating over the individual fibers along with the formation of a conducting layer covering the interfiber and interweave regions. This reduces the microwave-transparent spaces, resulting in the development of fabrics with efficient EMI shielding. The thin coating of polyaniline nanofibers over the fabrics helps to maintain the mechanical properties of the fabrics. Similarly, uniform coatings were also obtained for the polyaniline nanofiber graphite composite-based fabrics due to the use of the same synthesis procedure.

The EMI shielding efficiency of these materials can be analyzed by measuring their EMI shielding effectiveness (EMI SE) and is determined by the combination of the amounts of energy reflected (reflection shielding effectiveness ($SE_R$)) and absorbed (absorption shielding effectiveness ($SE_A$)) by the material during the transmission of the electromagnetic wave. Thus, the EMI SE is given as $SE_R+SE_A$, where $SE_R$ and $SE_A$ can be calculated from the scattering parameters according to the following equations

$SE_R\ (dB) = -10 \log\ (1 - S_{11}^2)$ and $SE_A\ (dB) = -10 \log\ [(S_{12}^2)/(1 - S_{11}^2)]$, where $S_{11}$ and $S_{12}$ are scattering parameters.[57,58]

The frequency dependence of the EMI SE of the polyaniline nanofibers and their composite with a sample thickness of 1 mm in the X and Ku-band frequency ranges (8.2–12.4 and 12.4–18 GHz) is given in Figure 7. The shielding efficiency is greatly improved by the addition of graphite, which may be due to the increased conductivity of the composite. The EMI SE increases from 71–77 dB to 83–89 dB with the addition of graphite to the polyaniline nanofibers in the measured frequency range. The conductivity of the pure polyaniline nanofibers is approximately 18.5 S cm$^{-1}$, and it increases to 24 S cm$^{-1}$ by the addition of a very small amount of graphite (2.3 wt.%) to the polyaniline nanofiber matrix. The graphite, due to its good conducting nature and flake-like morphology, acts as a conducting link between the polyaniline nanofibers, which accelerates the charge transfer and leads to increased conductivity and good EMI shielding properties.[41] The EMI SE of polyaniline nanofibers and their composite are almost constant in this frequency range and slightly increases with the frequency. The behavior, as well as the value of the EMI SE, depends on $SE_R$ and $SE_A$. The $SE_R$ and $SE_A$ performances of the polyaniline nanofibers and their composite in the frequency range of 8.2–18 GHz are also depicted in Figure 7. The $SE_R$ of these composites is found to decrease with the frequency, while that of $SE_A$ shows an increasing trend with the frequency. The addition of graphite filler leads to an increase in both $SE_R$ and $SE_A$, similar to the EMI SE.

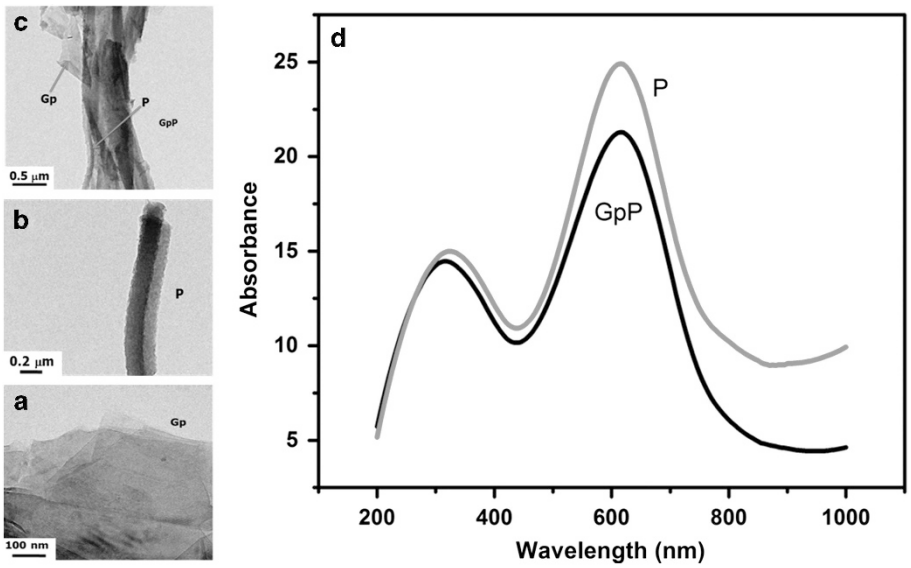


**Figure 3** Transmission electron microscope of (**a**) graphite, (**b**) polyaniline nanofibers (P) and (**c**) polyaniline nanofiber graphite composite (GpP) and (**d**) solid-state ultraviolet–visible spectra of polyaniline nanofibers and their graphite composite. A full color version of this figure is available at *Polymer Journal* online.

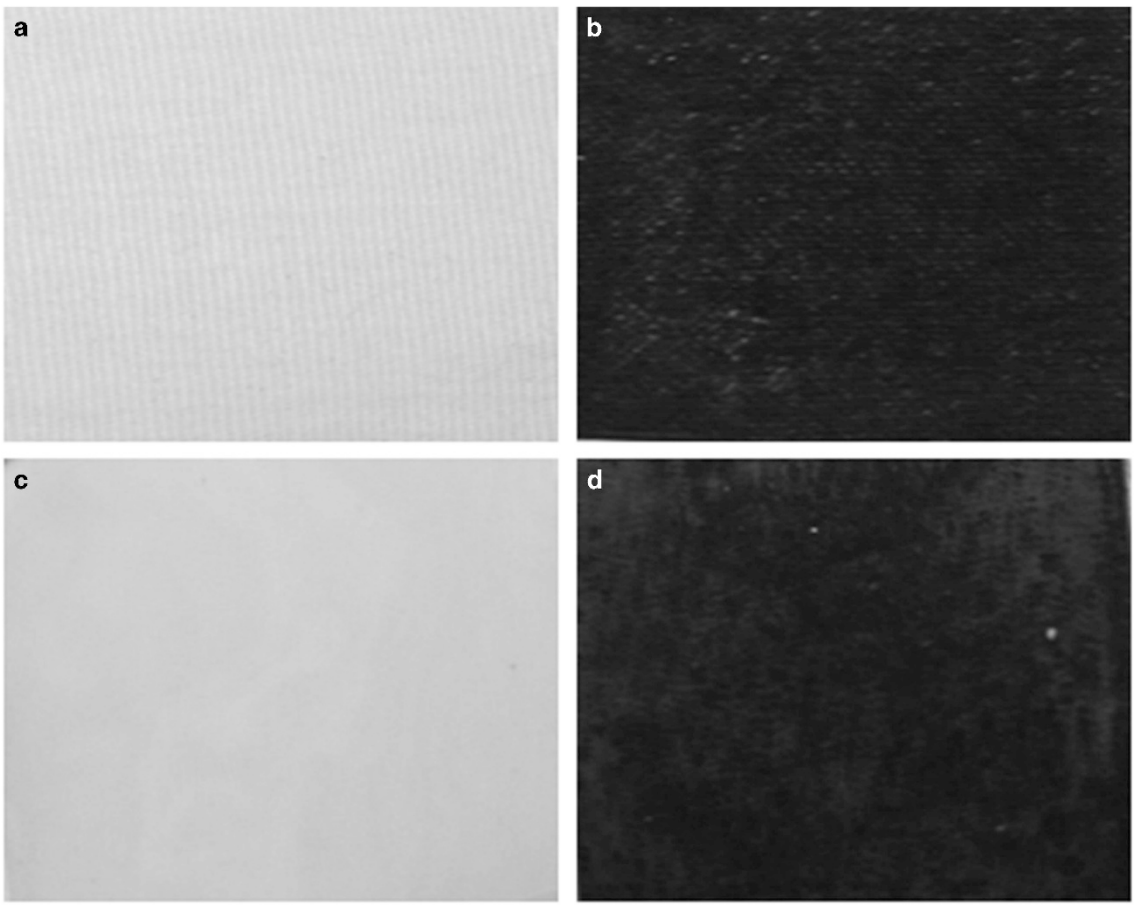


**Figure 4** Photographic images of (**a**) pure and (**b**) polyaniline nanofiber-based cotton and (**c**) pure and (**d**) polyaniline nanofiber-based nylon fabrics. A full color version of this figure is available at *Polymer Journal* online.

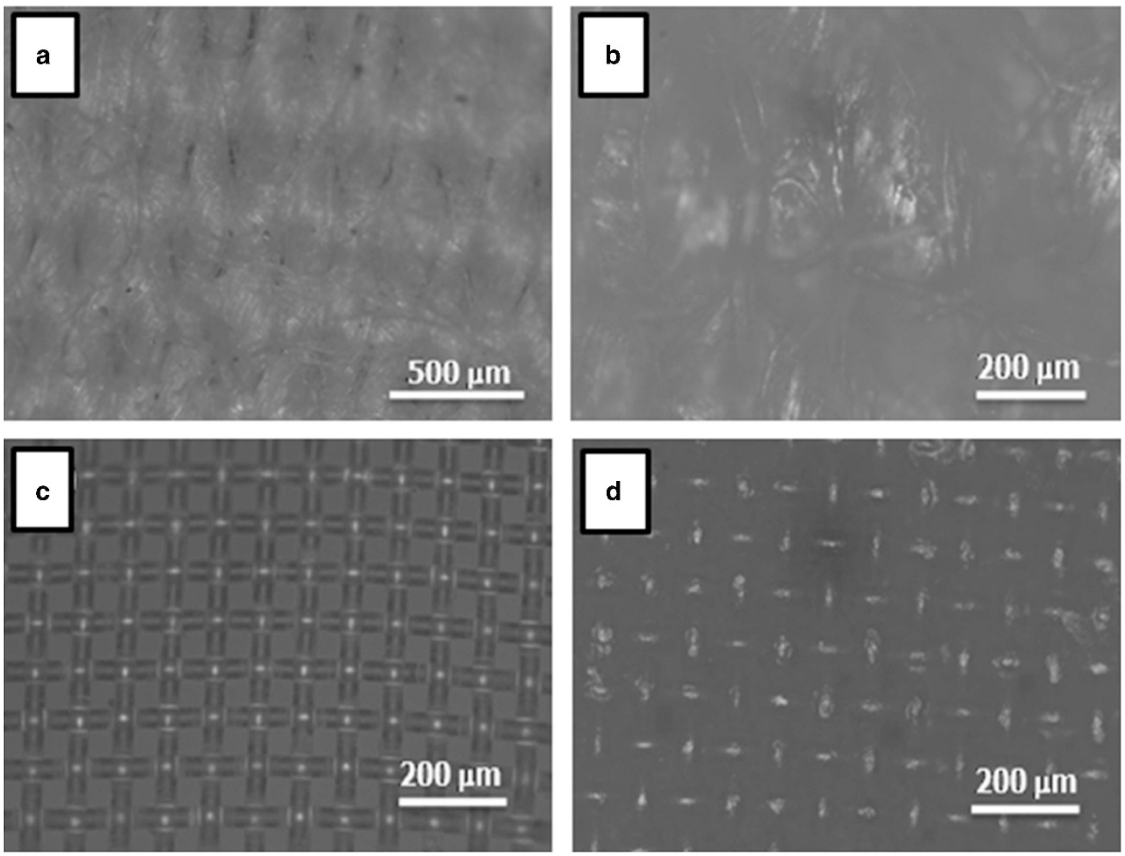


**Figure 5** Optical images of (**a**) pure and (**b**) polyaniline nanofiber-based cotton and (**c**) pure and (**d**) polyaniline nanofiber-based nylon fabrics. A full color version of this figure is available at *Polymer Journal* online.

The $SE_R$ value of the polyaniline nanofiber graphite composite is found to be in the range of 18–13 dB, while that of the polyaniline nanofibers is 14–10 dB in this frequency range. Similarly, with the addition of graphite, the $SE_A$ value increases from 57–67 to 65–76 dB in the measured frequency range. It is found that the polyaniline nanofibers and their graphite composite exhibit an attractive EMI shielding response for a small sample thickness of 1 mm with a significant contribution from $SE_A$. The solid-state absorption spectra of the polyaniline nanofibers indicate the presence of localized polarons that will interact with the incident electromagnetic radiation, leading to EMI shielding by absorption.[47] The presence of graphite improves the absorption-dominated shielding of the polyaniline nanofibers due to its conducting nature and flake-like morphology.[41] Hence, the absorption-dominated EMI shielding of the polyaniline nanofibers and their graphite composite is due to the combined effect of the conductivity of the composite, the measurement frequency range of GHz, and the morphologies of the polyaniline nanofibers and graphite, as well as the millimeter-range thickness of the shielding material.[52,59–62] The excellent EMI shielding properties of the polyaniline nanofibers and their graphite composite can attenuate nearly 100% of the EMI, making them attractive for many practical applications.

The shielding properties of the pristine cotton and nylon fabrics and the polyaniline nanofiber and composite-based fabrics are shown in Figure 8. The EMI SE values of both the pristine nylon and cotton fabrics of 0.1 mm thickness are negligible. Thin fabrics with an EMI shielding in the range of 11–15 dB are obtained with the growth of pure and graphite filler supplemented polyaniline nanofibers on these fabrics. The highest EMI shielding ability is shown by the polyaniline nanofiber graphite composite-based fabrics due to the relatively high EMI SE of the composite, as shown in Figure 7. A one hundred-fold increase in the EMI SE is observed with the formation of polyaniline nanofibers and their composites on cotton and nylon fabrics. The variation of the $SE_R$, as well as the $SE_A$ of these cotton and nylon fabrics with the frequency, is also shown in Figure 8. These fabrics are also found to shield mainly by absorption, similar to the polyaniline nanofibers and their composite. The $SE_R$ of the polyaniline nanofiber-based fabrics (both nylon and cotton) in the measured frequency range is 3 dB, and the $SE_A$ is 8–9 dB. The values of the above parameters for the polyaniline nanofiber graphite composite-based fabrics are 4 and 10–11 dB, respectively. Thus, thin EMI shielding cotton and nylon fabrics of approximately 0.1 mm thickness that can attenuate the EMI by approximately 97% are achieved, and they are superior to many of the reported polyaniline-based fabrics in the same frequency range with respect to the EMI SE, thickness and synthesis procedure.[22,23,31] The EMI SEs of these fabrics do not show considerable variation with the frequency. Moreover, the method of preparation of the polyaniline nanofiber-based fabrics is very simple, as the fabrics can be synthesized by an *in situ* polymerization method without any structure directing agent or organic solvent at room temperature. This is an added advantage from the techno-commercial and industrial viewpoint. Thin, flexible natural and synthetic fabrics

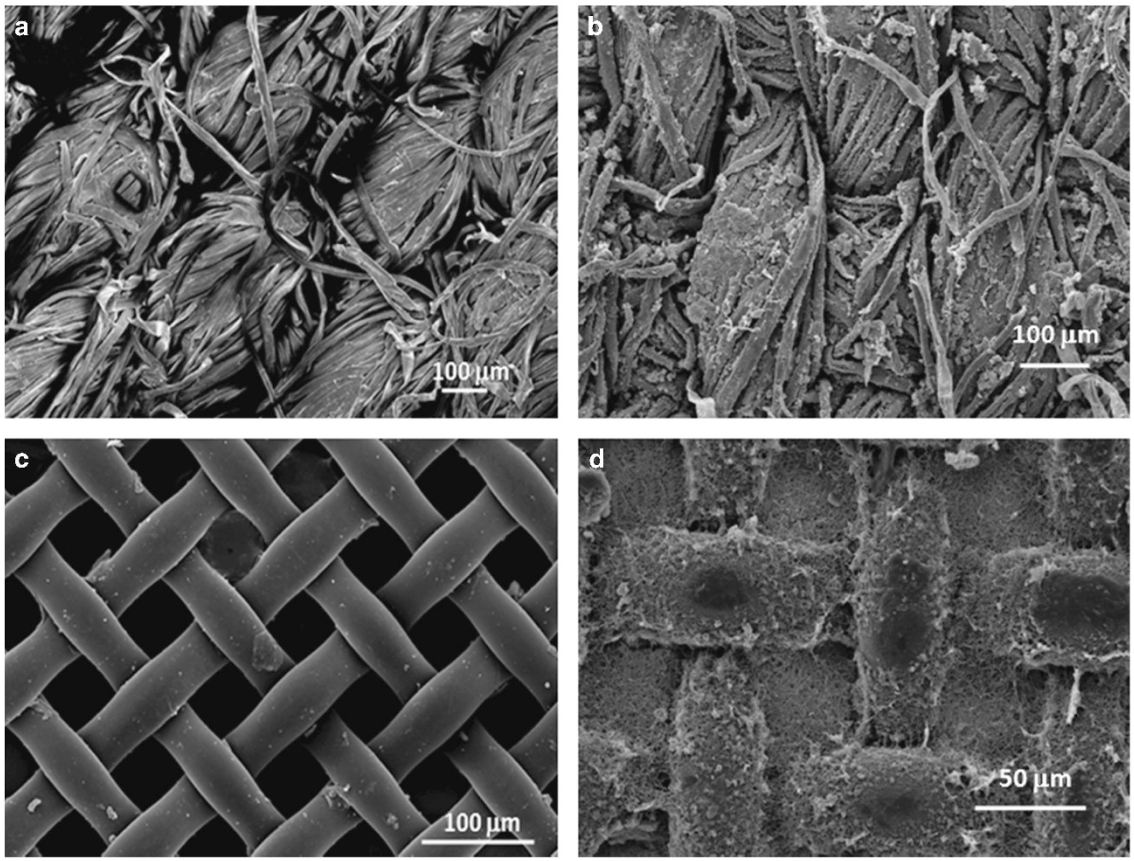


**Figure 6** SEM images of (**a**) pure and (**b**) polyaniline nanofiber-based cotton and (**c**) pure and (**d**) polyaniline nanofiber-based nylon fabrics.

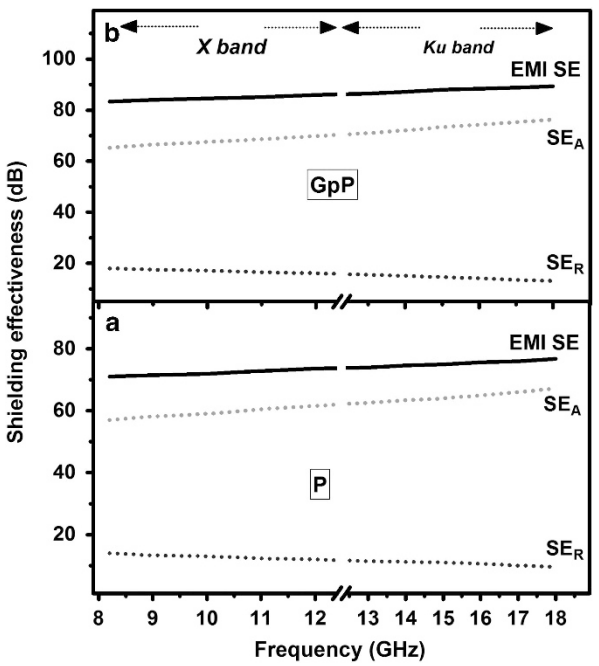


**Figure 7** Variation of EMI SE, $SE_A$ and $SE_R$ of (**a**) polyaniline nanofibers (P) and (**b**) polyaniline nanofiber graphite composite (GpP) of thickness 1 mm in the 8.2–18 GHz frequency range. A full color version of this figure is available at *Polymer Journal* online.

based on polyaniline nanofibers and their composite were prepared and can provide a stable wide bandwidth for shielding applications, particularly for ESD shielding applications.

## CONCLUSIONS

Flexible and lightweight EMI shields were developed by growing polyaniline nanofibers and their composite with graphite on cotton and nylon fabrics by an *in situ* polymerization method. The polyaniline nanofiber graphite composite was prepared by the addition of graphite flakes during polymerization with an aniline monomer–filler ratio of 4:1. The incorporation of the conducting filler results in the enhancement of the shielding properties of the polyaniline nanofibers and excellent EMI shielding in the range of 83–89 dB is obtained for the polyaniline nanofiber graphite composite over a wide frequency range of 8.2–18 GHz. The main shielding mechanism of the polyaniline nanofibers and their composite is absorption. The advanced fabrics that inherit the properties of the polyaniline nanofibers as well as those of the *in situ* incorporated conducting filler are thin (in the range of 0.1 mm) and exhibit EMI shielding in the range of 15 dB for polyaniline nanofiber graphite composite-based fabrics. Hence, flexible, thin, broadband shielding materials that can prevent approximately 97% of the EMI and are suitable for a broad range of shielding applications, particularly against ESD, have been successfully synthesized. These polyaniline nanofiber-based fabrics are prepared by a simple *in situ* polymerization route

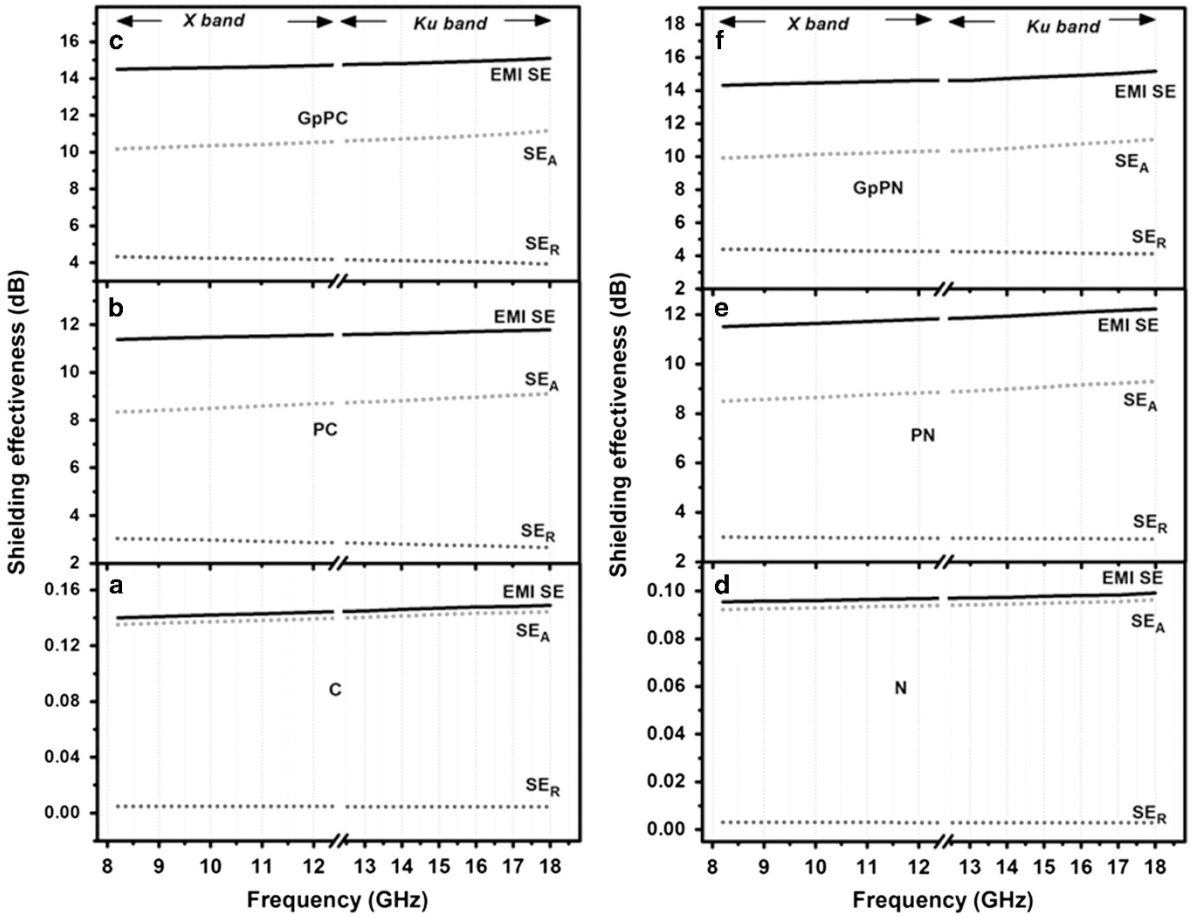


**Figure 8** Variation of EMI SE, $SE_A$ and $SE_R$ of (**a**) pure (C), (**b**) polyaniline nanofiber-based (PC), (**c**) polyaniline nanofiber graphite composite-based (GpPC) cotton fabrics and (**d**) pure (N), (**e**) polyaniline nanofiber-based (PN) and (**f**) polyaniline nanofiber graphite composite-based (GpPN) nylon fabrics of 0.1 mm thickness in the 8.2–18 GHz frequency range. A full color version of this figure is available at *Polymer Journal* online.

and can meet the growing demand for thin and flexible EMI shielding materials.

## CONFLICT OF INTEREST

The authors declare no conflict of interest.

## ACKNOWLEDGEMENTS

We are grateful to Mr Chandran and Mr Kiran Mohan of CSIR NIIST, Trivandrum, for the SEM and TEM analyses.

1 Weston, D. A. *Electromagnetic Compatibility: Principles and Applications* (Marcel Dekker, New York, United States, 2001).
2 Tong, X. C. *Advanced Materials and Design for Electromagnetic Interference Shielding* (CRC Press, Boca Raton, FL, USA, 2009).
3 Jagatheesan, K., Ramasamy, A., Das, A. & Basu, A. Electromagnetic shielding behaviour of conductive filler composites and conductive fabrics—a review. *Indian J. Fibre Text Res.* **39**, 329–342 (2014).
4 Wang, L. L., Tay, B. K. & See, K. Y. Electromagnetic interference shielding effectiveness of carbon based materials prepared by screen printing. *Carbon* **47**, 1905–1910 (2009).
5 Neelakandan, R., Giridev, V. R., Murugesan, M. & Madhusoothanan, M. Surface resistivity and shear characteristics of polyaniline coated polyester fabric. *J. Ind. Text* **39**, 175–186 (2009).
6 Cheng, K. B., Ueng, T. H. & Dixon, G. Electrostatic discharge properties of stainless steel/polyester woven fabrics. *Text. Res. J.* **71**, 732–738 (2001).
7 He, J., Li, R. & Gu, F. Preparation of polyaniline/nylon conducting fabric by layer by layer assembly method. *J. Appl. Polym. Sci.* **128**, 1673–1679 (2013).
8 Saini, P. & Choudhary, V. Conducting polymer coated textile based multilayered shields for suppression of microwave radiations in 8.2-12.4 GHz range. *J. Appl. Polym. Sci.* **129**, 2832–2839 (2013).
9 Jin, H., Chen, Q., Chen, Z., Hu, Y. & Zhang, J. Multi-LeapMotion sensor based demonstration for robotic refine tabletop object manipulation task. *CAAI Trans. Intell. Technol.* **1**, 104–113 (2016).
10 Gupta, K. K., Abbas, S. M. & Abhyankar, A. C. Ultra-lightweight hybrid woven fabric containing stainless steel/polyester composite yarn for total EMI shielding in frequency range 8–18 GHz. *J. Electromagnet. Wave* **29**, 1454–1472 (2015).
11 Shinagawa, S., Kumagai, Y. & Urabe, K. Conductive papers containing metallized polyester fibers for electromagnetic interference shielding. *J. Porous Mat.* **6**, 185–190 (1999).
12 Kumar, A., Singh, A. P., Kumari, S., Dutta, P. K., Dhawan, S. K. & Dhar, A. Polyaromatic-hydrocarbon-based carbon copper composites for the suppression of electromagnetic pollution. *J. Mater. Chem. A* **2**, 16632–16639 (2014).
13 Perumalraj, R. & Dasaradhan, B. S. Electroless nickel plated composite textile materials for electromagnet compatibility. *Indian J. Fibre Text. Res.* **36**, 35–41 (2011).
14 Gupta, T. K., Singh, B. P., Singh, V. N., Teotia, S., Singh, A. P., Elizabeth, I., Dhakate, S. R., Dhawan, S. K. & Mathur, R. B. $MnO_2$ decorated graphene nanoribbons with superior permittivity and excellent microwave shielding properties. *J. Mater. Chem. A* **2**, 4256–4263 (2014).
15 Song, W.-L., Guan, X.-T., Fan, L.-Z., Cao, W.-Q., Wang, C.-Y., Zhao, Q.-L. & Cao, M.-S. Magnetic and conductive graphene papers toward thin layers of effective electromagnetic shielding. *J. Mater. Chem. A* **3**, 2097–2107 (2015).
16 Qiang, R., Du, Y., Zhao, H., Wang, Y., Tian, C., Li, Z., Han, X. & Xu, P. Metal organic framework-derived Fe/C nanocubes toward efficient microwave absorption. *J. Mater. Chem. A* **3**, 13426–13434 (2015).
17 Gupta, T. K., Singh, B. P., Dhakate, S. R., Singh, V. N. & Mathur, R. B. Improved nanoindentation and microwave shielding properties of modified MWCNT reinforced polyurethane composites. *J. Mater. Chem. A* **1**, 9138–9149 (2013).

18 Kumar, R., Dhakate, S. R., Gupta, T., Saini, P., Singh, B. P. & Mathur, R. B. Effective improvement of the properties of light weight carbon foam by decoration with multi-wall carbon nanotubes. *J. Mater. Chem. A* **1**, 5727–5735 (2013).
19 Pawar, S. P., Marathe, D. A., Pattabhi, K. & Bose, S. Electromagnetic interference shielding through MWNT grafted $Fe_3O_4$ nanoparticles in PC/SAN blends. *J. Mater. Chem. A* **3**, 656–669 (2015).
20 Bonaldi, R. R., Siores, E. & Shah, T. Characterization of electromagnetic shielding fabrics obtained from carbon nanotube composite coatings. *Synthetic Met.* **187**, 1–8 (2014).
21 Song, W. L., Mao, S. C., Ming, M. L., Song, B., Chan, Y. W., Jia, L., Jie, Y. & Fan, L. Z. Flexible graphene/polymer composite films in sandwich structures for effective electromagnetic interference shielding. *Carbon* **66**, 67–76 (2014).
22 Kumar, N. M. & Thilagavathi, G. Surface resistivity and EMI shielding effectiveness of polyaniline coated polyester fabric. *J. Textile Apparel Technol. Manage.* **7**, 1–6 (2012).
23 Abbasi, A. M. R. & Militky, J. EMI shielding effectiveness of polypyrrole coated glass fabric. *J. Chem. Chem. Eng.* **7**, 256–259 (2013).
24 He, Q., Yuan, T., Zhang, X., Yan, X., Guo, J., Ding, D., Khan, M. A., Young, D. P., Khasanov, A., Luo, Z., Liu, J., Shen, T. D., Liu, X., Wei, S. & Guo, Z. Electromagnetic field absorbing polypropylene nanocomposites with tuned permittivity and permeability by nanoiron and carbon nanotubes. *J. Phys. Chem. C* **118**, 24784–24796 (2014).
25 Zhu, J., Wei, S., Haldolaarachchige, N., Young, D. P. & Guo, Z. Electromagnetic field shielding polyurethane nanocomposites reinforced with core-shell Fe-silica nanoparticles. *J. Phys. Chem. C* **115**, 15304–15310 (2011).
26 Guo, Z., Park, S., Hahn, H. T., Wei, S., Moldovan, M., Karki, A. B. & Young, D. P. Magnetic and electromagnetic evaluation of magnetic nanoparticle filled polyurethane nanocomposites. *J. Appl. Phys.* **101**, 09M511 (2007).
27 Chandrasekhar, P. *Conducting Polymers, Fundamentals and Applications: A Practical Approach* (Kluwer Academic, Dordrecht, Netherlands, 1999).
28 Saini, P., Choudhary, V., Vijayan, N. & Kotnala, R. K. Improved electromagnetic interference shielding response of poly(aniline)-coated fabrics containing dielectric and magnetic nanoparticles. *J. Phys. Chem. C* **116**, 13403–13412 (2012).
29 Skotheim, T. A., Elsenbaumer, R. L. & Reynolds, J. R. *Handbook of Conducting Polymers* (Marcel Dekker, New York, United States, 1998).
30 Joo, J. & Epstein, A. J. Electromagnetic radiation shielding by intrinsically conducting polymers. *Appl. Phys. Lett.* **65**, 2278–2280 (1994).
31 Saini, P., Choudhary, V. & Dhawan, S. K. Improved microwave absorption and electrostatic charge dissipation efficiencies of conducting polymer grafted fabrics prepared via *in-situ* polymerization. *Polym. Adv. Technol.* **23**, 343–349 (2012).
32 Wu, F., Xie, A., Sun, M., Wang, Y. & Wang, M. Reduced graphene oxide (RGO) modified spongelike polypyrrole (PPy) aerogel for excellent electromagnetic absorption. *J. Mater. Chem. A* **3**, 14358–14369 (2015).
33 Sivaram. *Polymer Science Contemporary Themes* (Tata McGraw-Hill, Noida, India, 1991).
34 Aldissi, M. *Intrinsically Conducting Polymers: An Emerging Technology* (Kluwer Academic, Dordrecht, Netherlands, 1993).
35 Skotheim, T. A. & Reynolds, J. R. *Handbook of Conducting Polymers. Third Edition: Conjugated Polymers—Processing and Applications* (CRC Press, Boca Raton, FL, USA, 2007).
36 Hakansson, E., Amiet, A., Nahavandi, S. & Kaynak, A. Electromagnetic interference shielding and radiation absorption in thin polypyrrole films. *Eur. Polym. J.* **43**, 205–213 (2007).
37 Trivedi, D. C. *Handbook of Organic Conductive Molecules and Polymers* (John Wiley & Sons Ltd, Chichester, UK, 1997).
38 Macdiarmid, A. G. Synthetic metals: a novel role for organic polymers. *Synthetic Met.* **125**, 11–22 (2002).
39 Abbas, S. M., Dixit, A. K., Chatterjee, R. & Goel, T. C. Preparation of nanosize polyaniline and its utilization for microwave absorber. *J. Nanosci. Nanotechnol.* **7**, 2129–2133 (2007).
40 Makeiff, D. A. & Huber, T. Microwave absorption by polyaniline–carbon nanotube composites. *Synthetic Met.* **156**, 497–505 (2006).
41 Joseph, N., Varghese, J. & Sebastian, M. T. Facile formulation and excellent electromagnetic absorption of room temperature curable polyaniline nanofiber based inks. *J. Mater. Chem. C* **4**, 999–1008 (2016).
42 Seshadri, D. T. & Bhat, N. V. Synthesis and properties of cotton fabrics modified with polypyrrole. *Sen'i Gakkaishi* **61**, 103–108 (2005).
43 dall'Acqua, L., Tonin, C., Peila, R., Ferrero, F. & Catellani, M. Performances and properties of intrinsic conductive cellulose-polypyrrole textiles. *Synthetic Met.* **146**, 213–221 (2004).
44 Kim, B., Koncar, V. & Dufour, C. Polyaniline-coated PET conductive yarns: study of electrical, mechanical and electro mechanical properties. *J. Appl. Polym. Sci.* **101**, 1252–1256 (2006).
45 Kyung, H. H., Kyung, W. O. & Tae, J. K. Polyaniline–nylon 6 composite fabric for ammonia gas sensor. *J. Appl. Polym. Sci.* **92**, 37–42 (2004).
46 Li, R., Liu, G., Gu, F., Zheng, W., Yang, S. & Jianqing, W. In situ polymerization of aniline on acrylamide grafted cotton. *J. Appl. Polym. Sci.* **120**, 1126–1132 (2011).
47 Joseph, N., Varghese, J. & Sebastian, M. T. Self-assembled polyaniline nanofibers with enhanced electromagnetic shielding properties. *RSC Adv.* **5**, 20459–20466 (2015).
48 Lee, K., Cho, S., Park, S. H., Heeger, A. J., Lee, C. W. & Lee, S. H. Metallic transport in polyaniline. *Nature* **441**, 65–68 (2006).
49 Tantawy, H. R., Aston, D. E., Smith, J. R. & Young, J. L. Comparison of electromagnetic shielding with polyaniline nanopowders produced in solvent-limited conditions. *ACS Appl. Mater. Interfaces* **5**, 4648–4658 (2013).
50 Fang, L., Zhang, X., Ma, J., Sun, D., Zhang, B. & Luan, J. Eco-friendly cationic modification of cotton fabrics for improving utilization of reactive dyes. *RSC Adv.* **5**, 45654–45661 (2015).
51 Duan, W., Xie, A., Shen, Y., Wang, X., Wang, F, Zhang, Y. & Li, J. Fabrication of superhydrophobic cotton fabrics with UV protection based on $CeO_2$ particles. *Ind. Eng. Chem. Res.* **50**, 4441–4445 (2011).
52 Aladpoosh, R., Montazer, M. & Samadi, N. In situ green synthesis of silver nanoparticles on cotton fabric using Seidlitzia rosmarinus ashes. *Cellulose* **21**, 3755–3766 (2014).
53 Fuan, H., Sienting, L., Helen, L. C. & Jintu, F. High dielectric permittivity and low percolation threshold in nanocomposites based on poly(vinylidene fluoride) and exfoliated graphite nanoplates. *Adv. Mater.* **21**, 710–715 (2009).
54 -Nia, Z. K., Montazer, M. & Latifi, M. Synthesis of nano copper/nylon composite using ascorbic acid and CTAB. *Colloids Surf. A Physiochem. Eng. Asp.* **439**, 167–175 (2013).
55 Montazer, M., Mozaffari, A. & Alimohammadi, F. Simultaneous dyeing and antibacterial finishing of nylon fabric using acid dyes and colloidal nanosilver. *Fibres Text. East. Eur.* **23**, 100–106 (2015).
56 Abdullah Dar, M., Kotnala, R. K., Verma, V., Shah, J., Siddiqui, W. A. & Alam, M. High magneto-crystalline anisotropic core-shell structured $Mn_{0.5}Zn_{0.5}Fe_2O_4$/polyaniline nanocomposites prepared by in situ emulsion polymerization. *J. Phys. Chem. C* **116**, 5277–5287 (2012).
57 Annapurna, D. & Sisir, K. D. *Microwave Engineering* (Tata McGraw Hill, Noida, India, 2009).
58 Joseph, N. & Sebastian, M. T. Electromagnetic interference shielding nature of PVDF-carbonyl iron composites. *Mater. Lett.* **90**, 64–67 (2013).
59 Stempien, Z., Rybicki, T., Rybicki, E., Kozanecki, M. & Szynkowska, M. I. In-situ deposition of polyaniline and polypyrrole electroconductive layers on textile surfaces by the reactive ink-jet printing technique. *Synthetic Met.* **202**, 49–62 (2015).
60 Guang, S. W., Xiao, J. Z., Yun, Z. W., Shuai, H., Lin, G. & Mao, S. C. Polymer composites with enhanced wave absorption properties based on modified graphite and polyvinylidene fluoride. *J. Mater. Chem. A* **1**, 7031–7036 (2013).
61 Zongping, C., Chuan, X., Chaoqun, M., Wencai, R. & Hui, M. C. Lightweight and flexible graphene foam composites for high-performance electromagnetic interference shielding. *Adv. Mater.* **25**, 1296–1300 (2013).
62 Singh, A. P., Mishra, M., Sambyal, P., Gupta, B. K., Singh, B. P., Chandrad, A. & Dhawan, S. K. Encapsulation of $\gamma$-$Fe_2O_3$ decorated reduced graphene oxide in polyaniline core–shell tubes as an exceptional tracker for electromagnetic environmental pollution. *J. Mater. Chem. A* **2**, 3581–3593 (2014).